Zoomorphology (2007) 126:245–264
DOI 10.1007/s00435-007-0044-2

ORIGINAL PAPER

Comparative immunohistochemistry of the cerebral ganglion in Gastrotricha: an analysis of FMRFamide-like immunoreactivity in *Neodasys cirritus* (Chaetonotida), *Xenodasys riedli* and *Turbanella* cf. *hyalina* (Macrodasyida)

Rick Hochberg

Received: 7 December 2006 / Accepted: 24 September 2007 / Published online: 18 October 2007

Abstract The neuropeptide FMRFamide (Phe–Met–Arg–Phe–NH_2) is part of a large and diverse family of peptidergic neurotransmitters present throughout the animal kingdom. To date, no such neuropeptides have been demonstrated in gastrotrichs despite their presence in closely related invertebrates such as nematodes. Here, the FMRFamidergic nervous system of three marine gastrotrichs is investigated with immunofluorescence, CLSM, and 3D computer imaging to gain insight into structure of the cerebral ganglion and test various phylogenetic hypotheses on its organization. Results reveal that FMRFamide-like immunoreactivity (IR) is present throughout the nervous systems of three species: *Neodasys cirritus* (Chaetonotida), *Xenodasys riedli* and *Turbanella* cf. *hyalina* (Macrodasyida). Both macrodasyidans possess FMRFamide-like IR in the central, peripheral- and stomatogastric-nervous systems, while FMRFamide-like IR is restricted to the CNS in *N. cirritus*. In all three species, the cerebral ganglion is dumbbell-shaped and bordered bilaterally by cerebral perikarya: numerous perikarya are present in *X. riedli* and *N. cirritus*, while few perikarya are present in *T.* cf. *hyalina*. Cerebral perikarya flank the nerve ring neuropil, which contains IR fibers in the supra- and subpharyngeal commissures of both macrodasyidans, but in *N. cirritus*, only contains IR fibers in the suprapharyngeal commissure. Together, these results confirm the peripharyngeal nature of the gastrotrich cerebral ganglion, but are equivocal on hypotheses of its tripartite structure. Still, the neural organization of gastrotrichs, in particular, the architecture of the cerebral ganglion, is expected to hold valuable information for future assessments of gastrotrich phylogeny, and may yet provide key insights into the evolution of this enigmatic taxon.

Keywords Confocal · Nerves · Gastrotricha · Neurotransmitter

R. Hochberg (✉)
University of Massachusetts Lowell,
One University Avenue, Lowell, MA 01854, USA
e-mail: rick_hochberg@uml.edu

Introduction

Gastrotricha is a small taxon of microscopic worm-like invertebrates characteristic of marine and freshwater environments, with most marine species living among the interstitial spaces between grains of sand. The miniscule size of gastrotrichs has generally impeded comparative investigations of several organ systems, with the exception of the myoepithelial pharynx (Ruppert 1982), the Y-cell system (Travis 1983) and the muscular system (Hochberg and Litvaitis 2001). Understandably, the complexity of some organ systems such as the nervous system are not easily studied, so much of what is known about the nervous system is described from studies of relatively few species (Teuchert 1976, 1977; Gagné 1980; Joffe and Kotikova 1987; Ruppert 1991; Joffe and Wikgren 1995; Wiedermann 1995; Hochberg and Litvaitis 2003; Liesenjohann et al. 2006). Still, these details have provided an intriguing view of the nervous system and its associated sensory devices. In general, the gastrotrich nervous system can be divided into three components: the CNS consists of a circumpharyngeal cerebral ganglion and paired (or multiple) nerve cords; the stomatogastric nervous system (SNS) consists of neurons that innervate the myoepithelial pharynx and intestine; and the peripheral nervous system (PNS) consists of neurites that innervate various sensory devices in the head and trunk regions. Most of the observations on these neural components

come from ultrastructural investigations (e.g., Teuchert 1977; Gagné 1980; Ruppert 1991; Wiedermann 1995; Hochberg and Litvaitis 2003; Liesenjohann et al. 2006), with comparatively fewer observations deriving from histochemical studies (Joffe and Kotikova 1987; Joffe and Wikgren 1995; Hochberg and Litvaitis 2003; Liesenjohann et al. 2006).

Histochemistry has the potential to reveal the composition of individual cells in the gastrotrich nervous system, e.g., neurotransmitters and neural proteins, but perhaps more importantly, it can also reveal the overall organization of the nervous system, which is difficult to visualize in microscopic animals. Organizational aspects such as the topology of cerebral perikarya, the structure of neural circuits, or patterns of innervation may provide unique insights into gastrotrich anatomy and evolution, and when combined with immunoreagents, may reveal patterns of neurotransmitter distribution that can provide clues to neural physiology and behavior. To date, few histochemical studies have been performed on gastrotrichs (Joffe and Kotikova 1987; Joffe and Wikgren 1995; Hochberg and Litvaitis 2003; Liesenjohann et al. 2006), but despite this paucity, these studies have revealed some interesting aspects of neural organization. In particular, catecholaminergic and serotonergic neurons are found throughout the cerebral ganglion and nerve cords (see Joffe and Kotikova 1987; Joffe and Wikgren 1995; Hochberg and Litvaitis 2003), and proteins such as tubulin and neurofilament contribute to the structure of the cerebral ganglion and some sensory devices (Hochberg and Litvaitis 2003; Liesenjohann et al. 2006).

Histochemical studies (e.g., Hochberg and Litvaitis 2003; Liesenjohann et al. 2006) have also corroborated ultrastructural observations of the gastrotrich CNS (e.g., Teuchert 1977; Wiedermann 1995), which found differences between the dorsal and ventral aspects of the cerebral neuropil. These differences, in combination with additional observations of cerebral organization, form the basis of two phylogenetic hypotheses that have broad implications for understanding metazoan phylogeny. For example, the Cycloneuralia *sensu* Nielsen 1995 is a phylogenetic hypothesis based in part on similarities in circumpharyngeal brain organization among six traditional "aschelminth" taxa: Gastrotricha, Nematoda, Nematomorpha, Priapula, Kinorhyncha, and Loricifera. This hypothesis proposes that a tripartite (perikarya–neuropil–perikarya) circumpharyngeal brain is a synapomorphy of Cycloneuralia. Alternatively, Schmidt-Rhaesa (1996) proposes that Gastrotricha is the sister group to a more inclusive Cycloneuralia *sensu strictu* (the remaining five phyla), and that the gastrotrich brain has a slightly different, and perhaps more plesiomorphic, organization, with an equal distribution of perikarya around the neuropil (see, Wiedermann 1995). The structure of the neuropil itself, with a thick suprapharyngeal commissure and thin subpharyngeal commissure, is proposed to be autapomorphic to Gastrotricha. While the inclusiveness of taxa within Cycloneuralia may be debatable, the clade itself receives good morphological support (Nielsen 1995; Schmidt-Rhaesa 1996); the clade is however, unsupported by molecular sequence data that generally attests to its paraphyletic nature within the Ecdysozoa (Garey 2001).

In an effort to provide further details on the organization of the cerebral ganglion in gastrotrichs, and assess its utility in studies of phylogeny, I have applied a combination of immunohistochemistry, confocal laser scanning microscopy (CLSM), and 3D computer imaging to visualize general cerebral architecture in two presumed primitive members of the Gastrotricha: *Neodasys cirritus* Evans, 1992 (Chaetonotida) and *Xenodasys riedli* (Schoepfer-Sterrer, 1969) (Macrodasyida). A third more derived species of Macrodasyida, *Turbanella* cf. *hyalina* Schulze, 1853, is also studied for comparison. Specifically, anti-FMRFamide (Phe–Met–Arg–Phe–NH_2) antibodies and indirect immunofluorescence are used to visualize the topology of cerebral perikarya relative to the neuropil—this information is used to test the aforementioned hypotheses on the tripartite organization of the gastrotrich brain. The cardioexcitatory peptide, FMRFamide, is used in this study because of its widespread expression in neuronal tissues of nearly all animals (e.g., Price and Greenberg 1977; Grimmelikhuijzen 1983; Lehman and Price, 1987; Shaw et al. 1996; Nichols et al. 1999; Müller and Sterrer 2004; also reviewed in Krajniak 2005), as opposed to the more restricted expression of other neurotransmitters such as serotonin (5-hydroxytryptamine) (for Gastrotricha see Joffe and Wikgren 1995; Hochberg and Litvaitis 2003). This widespread expression, at least at the level of antibody recognition, is due in part to the conservative nature of the family of FMRFamide-like neuropeptides (FaRPs), which all contain an RFamide sequence at their C-termini (e.g., McVeigh et al. 2005). In this respect, immunohistochemical analysis of the gastrotrich nervous system will likely reveal cells (through cross-reactivity) that contain other RFamide-related neuropeptides (FaRPs), thereby providing a broader picture of the cerebral ganglion than can obtained with other antibodies showing greater specificity. In addition, details of general nervous system organization are provided to allow for comparative studies of more derived species that may be useful for future phylogenetic analyses.

Material and methods

All gastrotrichs were collected between March and August 2005. Specimens of *X. riedli* (Schoepfer-Sterrer, 1969) (Macrodasyida: Xenodasyidae) were collected from Capron shoals (N27°26.52′, W°8013.81′)—a shallow (~3 m) subtidal site approximately 3 miles off the coast of

Fort Pierce, Florida. Specimens of *N. cirritus* Evans, 1992 (Chaetonotida, Multitubulatina: Neodasyidae) and *T.* cf. *hyalina* Schulze, 1853 (Macrodasyida, Turbanellidae) were collected from Green Turtle Beach, a high-energy beach on South Hutchinson Island, Fort Pierce, Florida (N27°25.177′, W80°16.368′). All specimens were anaesthetized in 7.5% $MgCl_2$ and subsequently processed for immunofluorescence and electron microscopy.

For immunohistochemistry, specimens of *X. riedli* ($n = 15$), *T.* cf. *hyalina*. ($n = 6$), and *N. cirritus* ($n = 16$) were fixed in 4% paraformaldehyde in 0.1 M PBS for 24 h at 4°C. Specimens were rinsed (3×) over the course of 24 h in 0.1 M PBS and then placed in IT Signal Enhancer (Ingenta) for 1 h to minimize non-specific staining. Five specimens of *T. hyalina* and 12 specimens each of *C. riedli* and *N. cirritus* were transferred to anti-rabbit FMRFamide [Immunostar; 1:500 in PBT (0.1 M PBS plus 0.5% Triton X-100)] and placed in 1.5 ml centrifuge tubes at 4°C on an orbital shaker for 24 h. Two types of controls were used. One control included five specimens (*X. riedli*, $n = 2$; *T.* cf. *hyalina*, $n = 1$; *N. cirritus*, $n = 2$) that were omitted from the primary antibody. The second control included three specimens (*X. riedli*, $n = 1$; *N. cirritus*, $n = 2$) and the primary antibody subjected to preabsorption with the primary peptide (FMRFamide; Immunostar) for 24 h. In theory, both the specimens and the antibody must be preincubated with the primary peptide to eliminate all staining (Burry 2000). All specimens were next rinsed in 0.1 M PBS over 24 h and transferred goat anti-rabbit Alexa Fluor 546 (Sigma-Aldrich). Specimens were stained in the dark at 4°C and on an orbital shaker for 24 h and then rinsed in 0.1 M PBT for 24 h. All specimens were mounted in GelMount on glass slides.

Immunostained gastrotrichs were examined on a Nikon Eclipse E800 compound microscope equipped with a Biorad Radiance 2000 laser system at the Smithsonian Marine Station in Fort Pierce, Florida. Lasersharp software (v. 4.0) was used to collect a series of 0.05 or 0.1 µm optical sections with maximum intensity projection along the *z*-axis. Confocal images were imported into Confocal Assistant (v. 4.0) and made into TIF files. Additional digital files were imported into Volocity (Improvision) to render 3-D images and create *X-Y-Z* rotations (TIF, AVI files). No manipulations of the original images were made other than changes of color (false color or grayscale) or cropping. The program Carnoy V 2.0 (©2001 Peter Schols) was used to make measurements of neurons in some digital images.

Gastrotrichs were prepared for scanning electron microscopy (SEM) with the following protocol: (1) anaesthetization for 20 m in 7.5% $MgCl_2$; (2) primary fixation in 3% glutaraldehyde in 0.1 M cacodylate buffer (pH 7.2) for 24 h, (3) rinse four times (15 m each) and (4) postfix in 1% OsO_4 in 0.1 M cacodylate buffer for 1 h. Following four more buffer rinses (15 m each), gastrotrichs were dehydrated in a graded ethanol series, transferred to modified BEEM capsules, and dehydrated in a critical point dryer. Dehydrated specimens were sputter coated with gold and examined on a JEOL 6400 SEM at 10 kV. A single specimen of *Dactylopodola baltica* (Remane, 1926) was prepared for TEM. Following a similar fixation and dehydration protocol as above, with acetone replacing ethanol as the dehydrating agent, the specimen was embedded in Epon–Araldite and sectioned on a Sorvall ultramicrotome. Gold sections were stained with uranyl acetate and lead citrate and examined on a JEOL 100CX TEM at 60 kV.

Results

General aspects

Immunoreactivity (IR) to anti-FMRFamide is present throughout the central nervous system (CNS) of all species (Figs. 1, 2, 3, 4, 5, 6, 7, 8, 9, 10, 11, 12). Only the macrodasyidan gastrotrichs show IR in the PNS and SNS. For the purposes of this paper, the CNS consists of the cerebral ganglion (a bilateral cluster of perikarya positioned around a central neuropil) and major nerve cords that project off the cerebral ganglion; the PNS consists of perikarya and neurites that innervate the bodywall in the head and trunk regions; and the SNS consists of perikarya and neurites closely associated with the myoepithelial pharynx and intestine. It should be noted that the distinction between perikarya of the CNS and PNS in the head region is somewhat arbitrary due to the proximity of the cells of each system. Measurements of the cerebral ganglion are determined for a single specimen of each species for general comparative purposes. Measurements include: (1) the distance from the tip of the head to the most anterior dorsal commissure; (2) the width of the cerebral ganglion as measured from the distance between the most lateral cerebral perikarya; and (3) the length of the cerebral ganglion as measured from the most anterior commissure to the most posterior perikaryon. Negative control specimens showed no IR; preabsorption with the primary peptide negated antibody staining in the additional control specimens.

Xenodasys riedli (Macrodasyida: Xenodasyidae)

The CNS is defined by intense IR in the cerebral ganglion and posterior nerve cords (Figs. 1, 2, 3, 4). Measurements are taken from a single adult specimen approximately 300 µm in total body length. The cerebral ganglion is located approximately 33 µm from the tip of the head, just posterior of the large plate (lp) that covers the dorsal surface (Figs. 1a, c–f, 3a). The cerebral ganglion can be

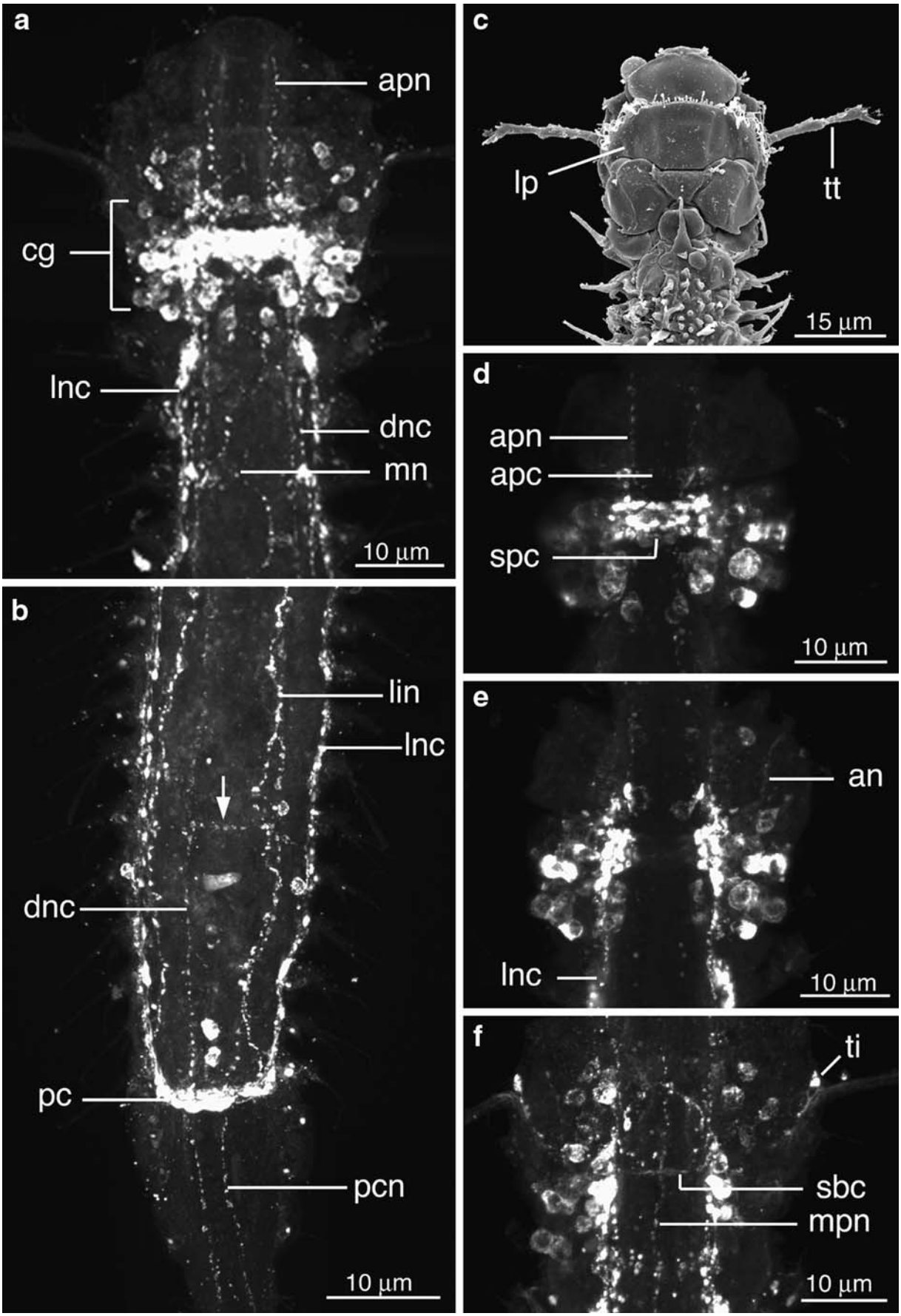
a
apn
cg
lnc
dnc
mn
10 µm
b
lin
lnc
dnc
pc
pcn
10 µm
c
lp
tt
15 µm
d
apn
apc
spc
10 µm
e
an
lnc
10 µm
f
ti
sbc
mpn
10 µm

◀ **Fig. 1** *Z*-projections of FMRFamide-like immunoreactivity (IR) in *Xenodasys riedli*. **a** IR in the head and anterior pharynx revealing the dorsal cerebral ganglion (*cg*) and several posterior nerves (333 × 0.1 µm optical slices). **b** IR in the posterior trunk region revealing the dorsal nerve cords (*dnc*), lateral nerve cords (*lnc*) and associated PNS nerves (249 × 0.05 µm optical slices). **c** SEM micrograph of the head region showing the large cuticular plate (*lp*) and head tentacles (*tt*). **d** IR in the dorsal region of the cerebral ganglion showing suprapharyngeal commissure (*spc*) (36 × 0.1 µm optical slices). **e** IR in the middle region of the cerebral ganglion (55 × 0.1 µm optical slices). **f** IR in the ventral region of the cerebral ganglion revealing the subpharyngeal commissure (sbc) and innervation of the myoepithelial pharynx (65 × 0.1 µm optical slices). *an* anterior neuron of the PNS, *apc* anterior pharyngeal commissure of the cerebral ganglion, *apn* anterior pharyngeal neuron of the SNS, *lin* lateral intestinal neuron of the SNS, *mn* medial neuron of the PNS, *mpn* medial pharyngeal neuron of the SNS, *pc* posterior commussure, *pcn* posterior neurite from the *pc*, *ti* tentacle innervation of the PNS

broadly divided into dorsal and ventral components. Dorsally, there are two commissures: a thin anterior pharyngeal commissure (2 µm diameter; apc, Figs. 1d, 4a, 5a) and a thick suprapharyngeal commissure (5–6 µm diameter; spc, Figs. 1d, 2, 3b, 5). The anterior commissure shows considerably weaker IR. The suprapharyngeal commissure is strongly convex (Fig. 2). A bilateral cluster of more than 20 perikarya is positioned on either side of the commissures, with few perikarya dorsal to the commissures (Figs. 1, 2, 3, 4, 5). Individual perikarya are oval in shape and approximately 3 µm wide by 5 µm long. Ventrally, there are a few perikarya positioned lateral to the subpharyngeal commissure (sbc; Fig. 5c). The subpharyngeal commissure shows weak IR but is present in all specimens.

Projecting off the cerebral ganglion are three pairs of thick nerve cords: one anterior pair and two posterior pairs. The anterior nerve cords (anc; Figs. 2b, 5) show weak IR and have few perikarya along their length; they parallel the myoepithelial pharynx for part of its length. The posterior nerve cords are present in dorsal (dnc) and lateral (lnc) positions (Figs. 1 a, b, 3b, 4 d, e, 5). The specific origins of the nerve cords within the cerebral ganglion cannot be determined. Both pairs of nerve cords project posteriorly along the trunk and have small swellings (perikarya?) along their length. A single thin commissure connects all four cords at the pharyngeointestinal junction (not shown) and again at approximately two-thirds body length (arrow; Fig. 1b). The dorsal nerve cords coalesce above the lateral nerve cords—the lateral nerve cords coalesce at a thick posterior commissure (pc; Figs. 1b, 4 c) approximately 80 µm from the posterior end and just anterior of the chordoid organ (ch). The posterior commissure is approximately 32 µm wide and 6 µm in diameter at its center.

The PNS and stomatogastric-nervous systems show intense IR throughout the body. The majority of IR in the PNS is localized in the head region, with several perikarya and neurites positioned anterior to the cerebral ganglion (Figs. 1a, f, 3b, 4b, 5). Anteriorly, a few dorsal and ventral perikarya are present close to the tip of the head and send neurites toward the buccal region (Figs. 1f, 4b, 5). A single pair of dorsal neurites (apn) projects off the anterior pharyngeal commissure and run the length of the pharynx (Figs. 1a, 4a). A single pair of ventral neurites (an) projects from either side of the cerebral ganglion and innervate the ventrolateral head region (Figs. 1e, 5). An additional pair of perikarya is present around the head tentacles and innervates them for part of their length (ti, Figs. 1f, 3, 5). A single wavy neurite also projects off the center of the suprapharyngeal commissure and innervates the trunk region (mn; Figs. 1a, f, 4a, 5a); this neurite is highly varicose and loses IR towards the posterior region of the pharynx. The site of innervation is unknown. Additionally, a pair of neurites (pcn) projects off the posterior commissure (pc) in the posterior body region (where the lnc coalesce) and parallels the chordoid organ for its entire length (Fig. 1b).

The SNS is well defined and clearly separate from the PNS; neurites of the SNS are always associated with the digestive tract and never project external to the pharynx or intestine. Three ventral longitudinal neurites run the length of the pharynx (Figs. 4b, 5): one medial pharyngeal neurite (mpn) and two lateral pharyngeal neurites (lpn). The two lateral neurites are interconnected by a ventral commissure (vc) just posterior of the subpharyngeal commissure (Figs. 4b, 5). Additional commissures may be present but IR is very weak and highly varicose. The median neurite appears to terminate at the base of the pharynx, while the lateral neurites project into the trunk region (as lateral intestinal neurites, lin) and run along the length of the digestive tract (Figs. 1b, 4c). These neurites connect to the posterior commissure in the trunk region.

Turbanella cf. *hyalina* (Macrodasyida: Turbanellidae)

The CNS shows strong IR within the cerebral ganglion and nerve cords (Figs. 6, 7). Unlike the condition in *X. riedli*, perikarya of the cerebral ganglion are closely associated with anterior cells of the PNS (Fig. 6a). Measurements are taken from a single adult specimen approximately 410 µm long; measurements of the cerebral ganglion (width) might be overestimates because of the close association with PNS cells. The cerebral ganglion is located approximately 30 µm from the tip of the head, is approximately 61 µm wide by 25 µm long, and consists of dorsal and ventral components. Dorsally, the center of the cerebral ganglion consists of three thin commissures: an anterior pharyngeal commissure (apc), a suprapharyngeal commissure (spc), and a posterior pharyngeal commissure (ppc) (Figs. 6, 8). The suprapharyngeal commissure is the thickest commissure

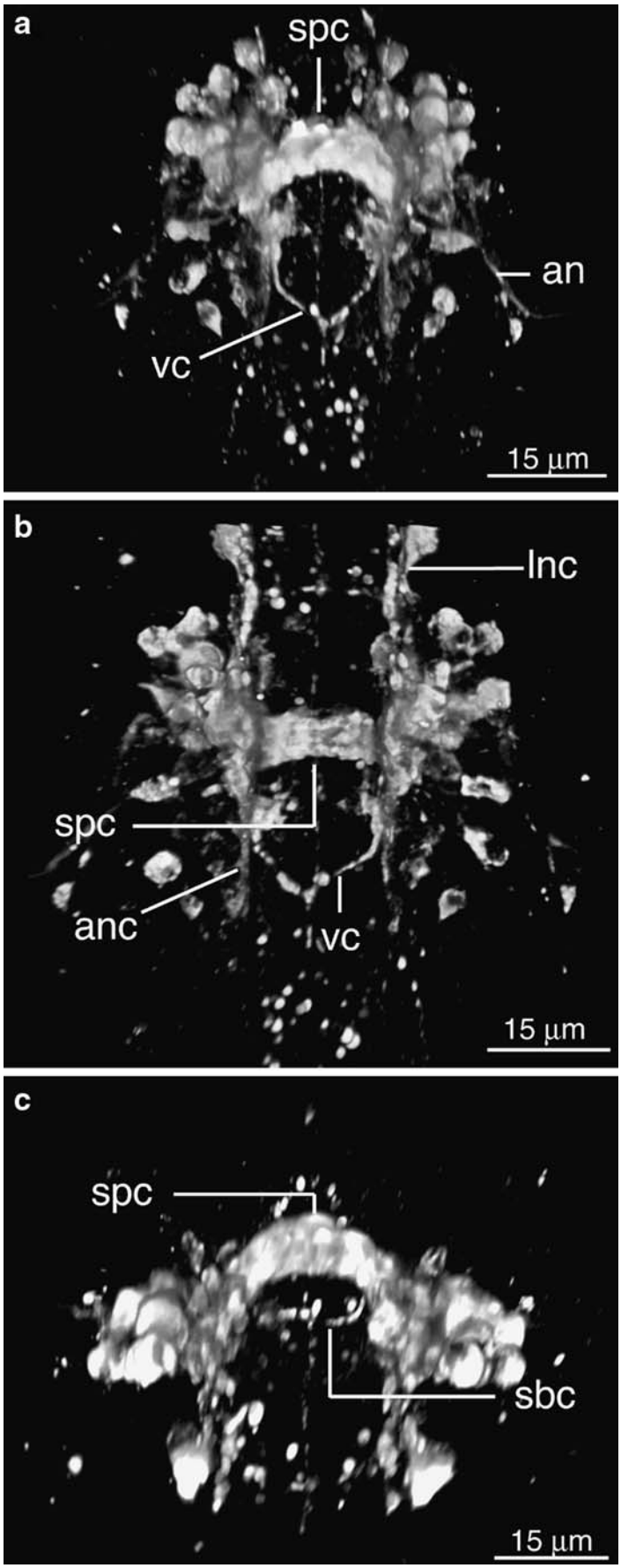

Fig. 2 Three-dimensional images of the cerebral ganglion of *Xenodasys riedli* based on FRMFamide-like IR. **a** Anterior view of the cerebral ganglion showing the suprapharyngeal commissuire (*spc*) of the cerebral ganglion and parts of the SNS and PNS. **b** Ventral view of the cerebral ganglion—anterior at the bottom. **c** Dorso-posterior view of the cerebral ganglion showing the major commissures. *an* anterior nerve of the PNS, *anc* anterior nerve cord of the CNS, *lnc* lateral nerve cord of the CNS, *sbc* subpharyngeal commissure, *vc* ventral commissure of the SNS

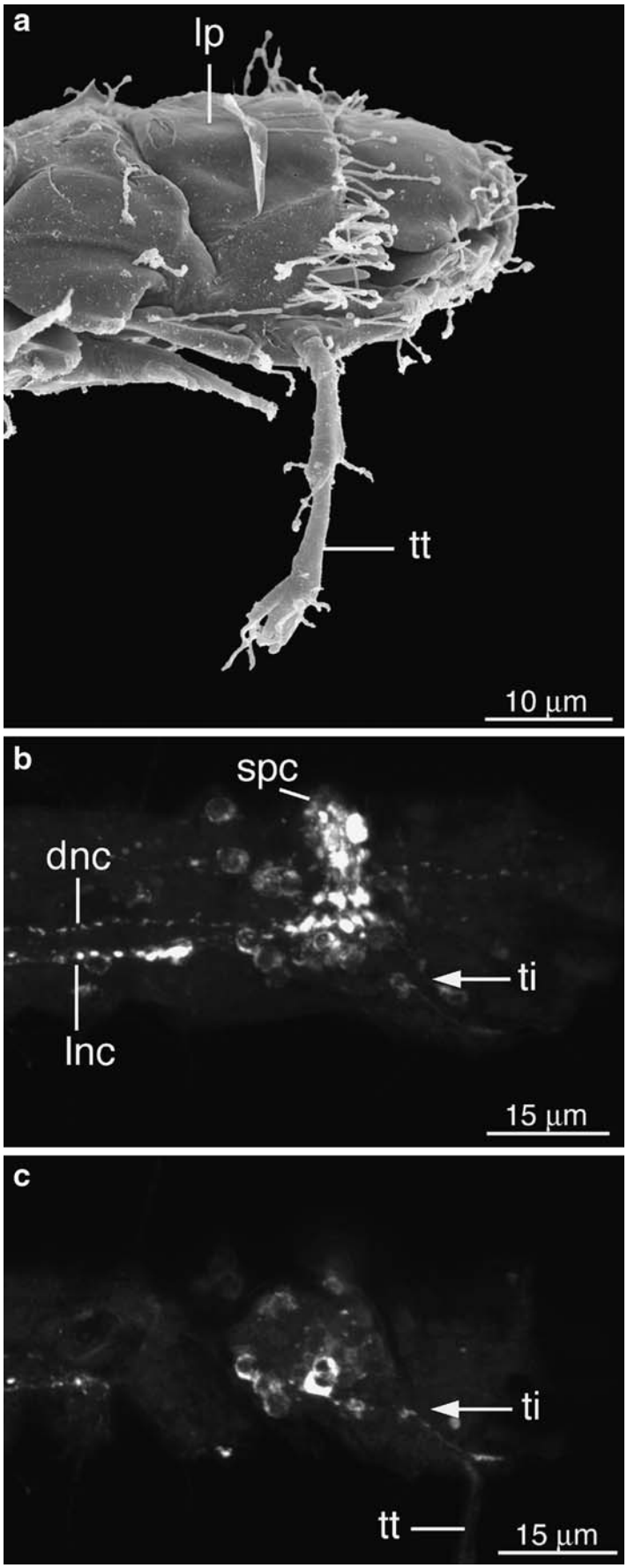

Fig. 3 Lateral views of the head of *Xenodasys riedli*. **a** SEM micrograph showing the large plate of the head (*lp*) and the sensory tentacles (*tt*). **b** Z-projection of FMRFamide-like IR—deep focus on right side of the cerebral ganglion revealing the suprapharyngeal commissure (*spc*), major nerve cords of the CNS, and perikaryon of the PNS (*ti*) that innervates the tentacles. 40 × 0.05 µm optical slices. **c** *Z*-projection of FMRFamide-like IR—shallow focus on the lateral head region revealing the neurite of the perikaryon (*ti*) that innervates the sensory tentacles (15 × 0.1 µm optical slices). *dnc* dorsal nerve cord, *lnc* lateral nerve cord

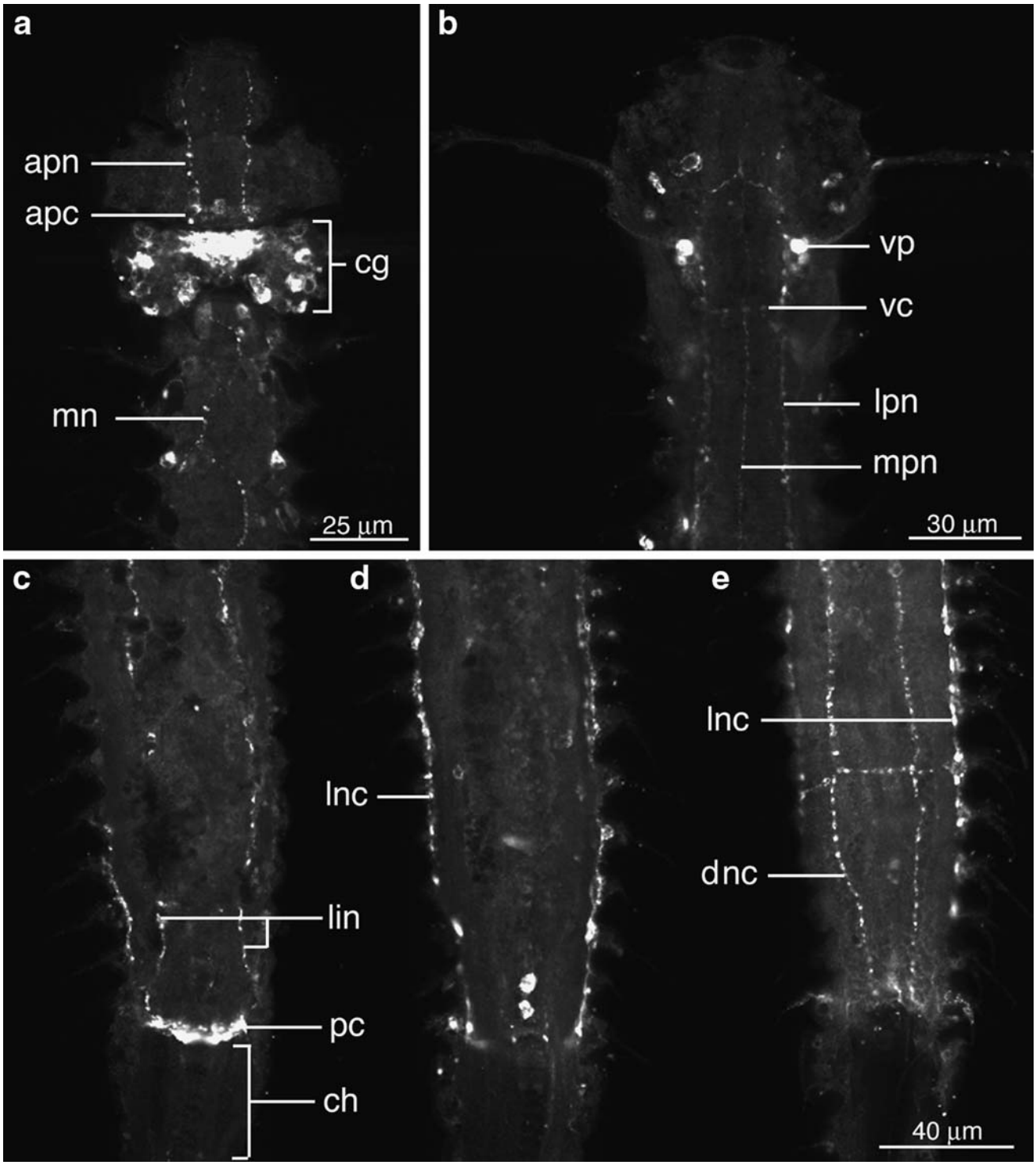

Fig. 4 *Z*-projections of the CNS and PNS of *Xenodasys riedli*. **a** Dorsal view of the anterior end showing the cerebral ganglion (*cg*), weakly IR anterior pharyngeal commissure (*apc*) of the cerebral ganglion, and parts of the PNS that innervate the myoepithelial pharynx. **b** Ventral view of the anterior end (same specimen) showing a single perikaryon (*vp*) associated with the base of the cerebral ganglion and elements of the PNS that innervate the myoepithelial pharynx. The subpharyngeal commissure is not in focus. **c–e** Successive views of IR in the posterior trunk region, from ventral to dorsal. Each image is 40 × 0.1 µm optical slices. *apn* anterior pharyngeal neuron of the SNS, *ch* region of the chordoid organ, *dnc* dorsal nerve cord of the CNS, *lin* lateral intestinal neuron, *lpn* lateral pharyngeal neuron of the SNS, *lnc* lateral nerve cord of the CNS, *mn* medial neuron of the PNS, *mpn* medial pharyngeal neuron of the SNS, *pc* posterior commissure, *vc* ventral commissure

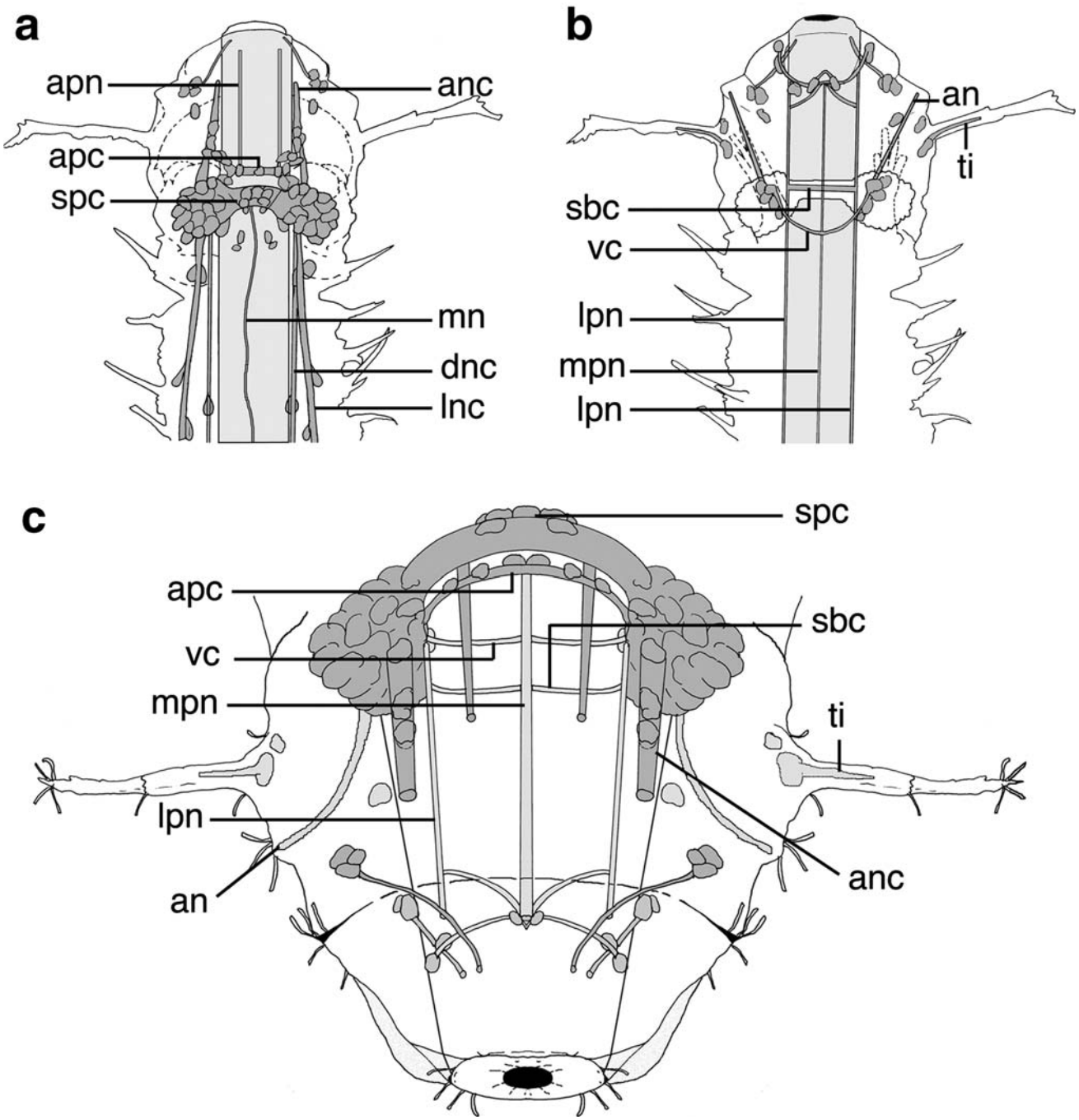

Fig. 5 Diagram of FMRFamide-like IR observed in *Xenodasys riedli*. **a** Dorsal view of the anterior end. **b** Ventral view of the anterior end. **c** 3D en face view of the anterior end. Dorsal cells and neurites are shaded darker than ventral cells and neurites in this illustration. *an* anterior neuron of the PNS, *anc* anterior nerve cord of the CNS, *apc* anterior pharyngeal commissure of the cerebral ganglion, *apn* anterior pharyngeal neuron of the SNS, *dnc* dorsal nerve cord of the CNS, *lpn* lateral pharyngeal neuron of the SNS, *lnc* lateral nerve cord of the CNS, *mn* medial neuron of the PNS, *mpn* medial pharyngeal neuron of the SNS, *sbc* subpharyngeal commissure of the cerebral ganglion, *spc* suprapharyngeal commissure of the cerebral ganglion, *ti* PNS innervation of the head tentacle, *vc* ventral commissure

and not well separated from the apc or ppc in all specimens (Fig. 8). The lateral perikarya of the cerebral ganglion are not particularly well defined, and there is a large amount of IR despite the presence of less than five perikarya total per side (Fig. 6b, d). Two perikarya are present posterior of the ppc; these perikarya appear to send short neurites to the larger IR mass of cerebral perikarya on either side of the cerebral ganglion (Fig. 8). In addition, at least one perikaryon on each side of the head innervates the lateral body wall (Fig. 6d). Ventrally, there is a pair of bilateral

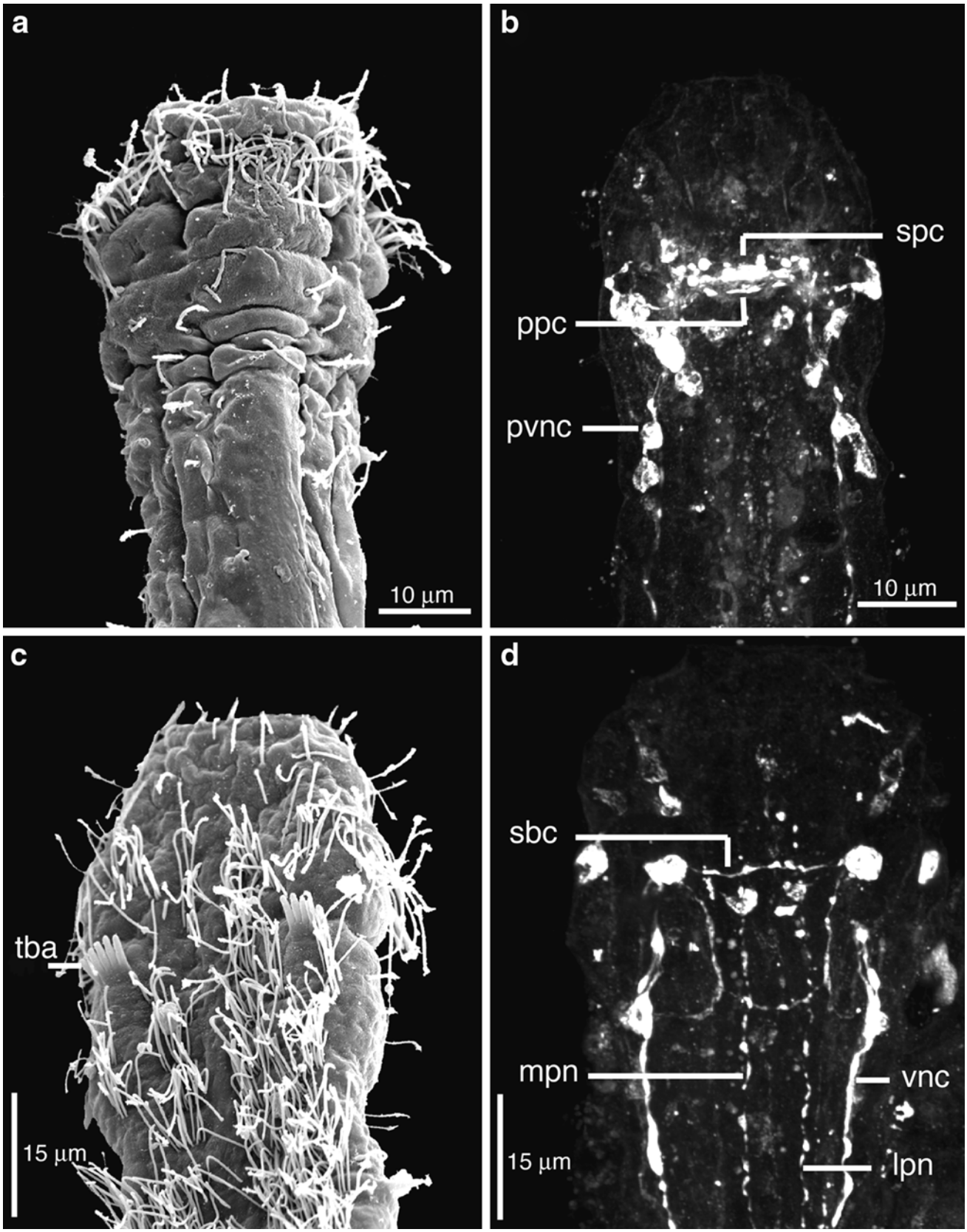
a
10 µm
b
spc
ppc
pvnc
10 µm
c
tba
15 µm
d
sbc
mpn
vnc
15 µm
lpn

◀ **Fig. 6** SEM and confocal views of the anterior end of *Turbanella* cf. *hyalina* aligned for comparison. **a** SEM of the dorsal region of the head. **b** *Z*-projection of FMRFamide-like IR in the dorsal region of the head showing portions of the CNS (51 × 0.1 µm optical slices). **c** SEM of the ventral region of the head. **d** *Z*-projection of FMRFamide-like IR in the ventral region of the head showing portions of the CNS and SNS (same specimen as in **b**) 40 × 0.1 µm optical slices. *lpn* lateral pharyngeal neuron of the SNS, *mpn* medial pharyngeal neuron of the SNS, *ppc* posterior pharyngeal commissure of the cerebral ganglion, *pvnc* perikarya of the ventral nerve cord of the CNS, *sbc* subpharyngeal commissure of the cerebral ganglion, *spc* suprapharyngeal commissure of the cerebral ganglion, *tba* anterior adhesive tubes, *vnc* ventral nerve cord of the CNS

perikarya on either side of the subpharyngeal commissure (sbc); the subpharyngeal commissure has weak IR and is very thin (ca. 1 µm diameter) (Fig. 6d). A second pair of ventral perikarya is present close the midline; these cells send short neurites towards the first pair of ventral perikarya.

Two pairs of nerve cords project off the cerebral ganglion (Figs. 6b, d, 7, 8). The anterior nerve cords (anc) project from the ventral region of the cerebral ganglion forward about 15 µm (not shown). These nerve cords are closely associated with several perikarya at their anterior end (see below). Posteriorly, a pair of ventral nerve cords (vnc) projects into the trunk region and coalesce at the posterior end (Fig. 7b). The posterior commissure is not well defined. Several perikarya are closely associated with the nerve cords along their length, especially at a site close to the anterior adhesive tubes (Fig. 6c, d).

The PNS of the head consists of perikarya and neurites closely associated with the cerebral ganglion (Figs. 6, 8). Anteriorly, several ventral perikarya are present at the tip of the anterior nerve cords and may innervate the dorsal and lateral body wall; the lateral body wall is the site where a tuft of sensory cilia is present. Because of the compression of the coverslip in most specimens, it is difficult to determine with accuracy if these perikarya unequivocally innervate the ciliary tufts or a region close to the cilia. The only other well-defined IR in the PNS is present is a medial neurite (mn) that projects off the suprapharyngeal commissure (not shown, but see Fig. 8). This neurite has extremely weak IR.

The SNS is well defined and quite complex (Figs. 6d, 7b, 8). The SNS consists of several longitudinal neurites connected by a series of commissures throughout the pharynx. Five longitudinal neurites run the length of the pharynx.

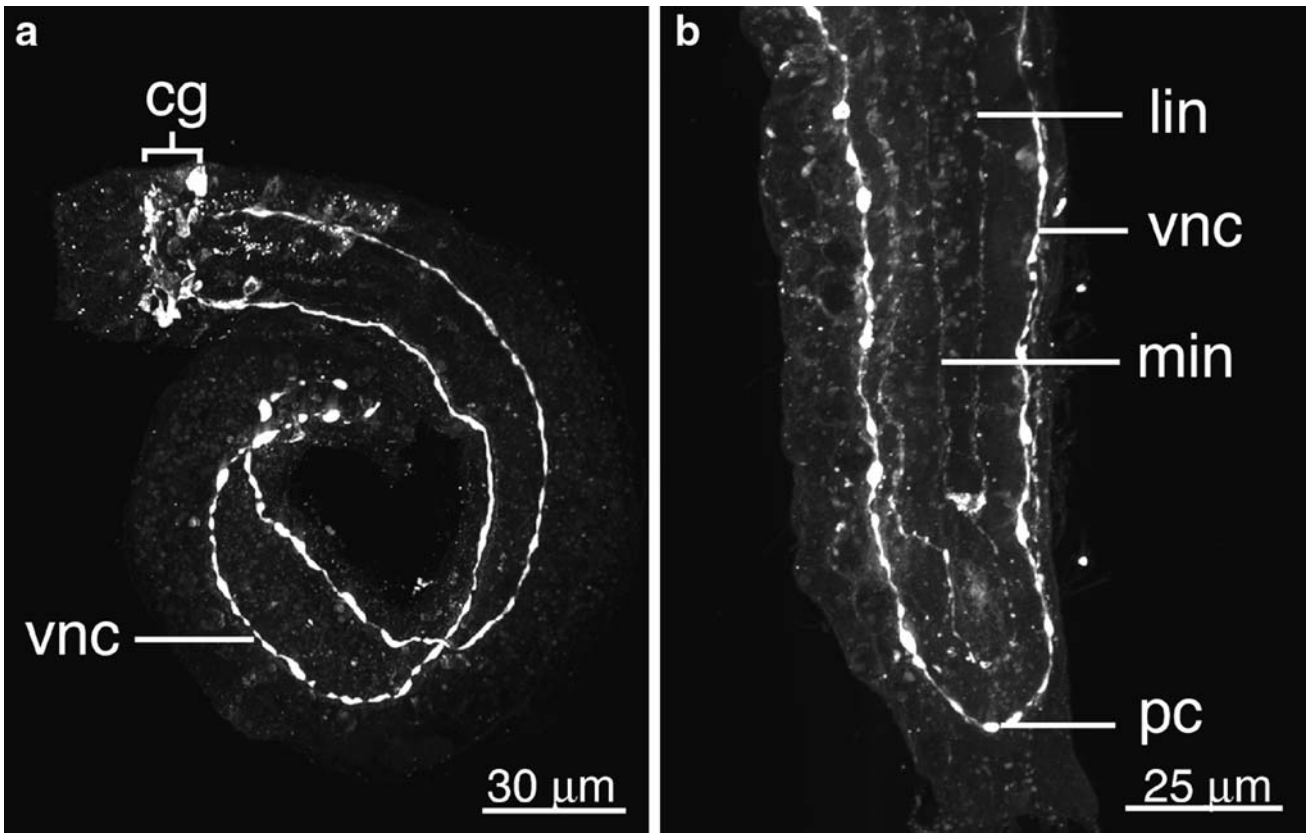

Fig. 7 *Z*-projections of FMRFamide-like IR in *Turbanella* cf. *hyalina*. **a** Whole specimen. 95 × 0.1 µm optical slices. **b** Ventral view of the posterior region (195 × 0.1 µm optical slices). *cg* cerebral ganglion, *lin* lateral intestinal neuron of the SNS, *min* medial intestinal neuron of the SNS, *pc* posterior commissure, *vnc* ventral nerve cord of the CNS

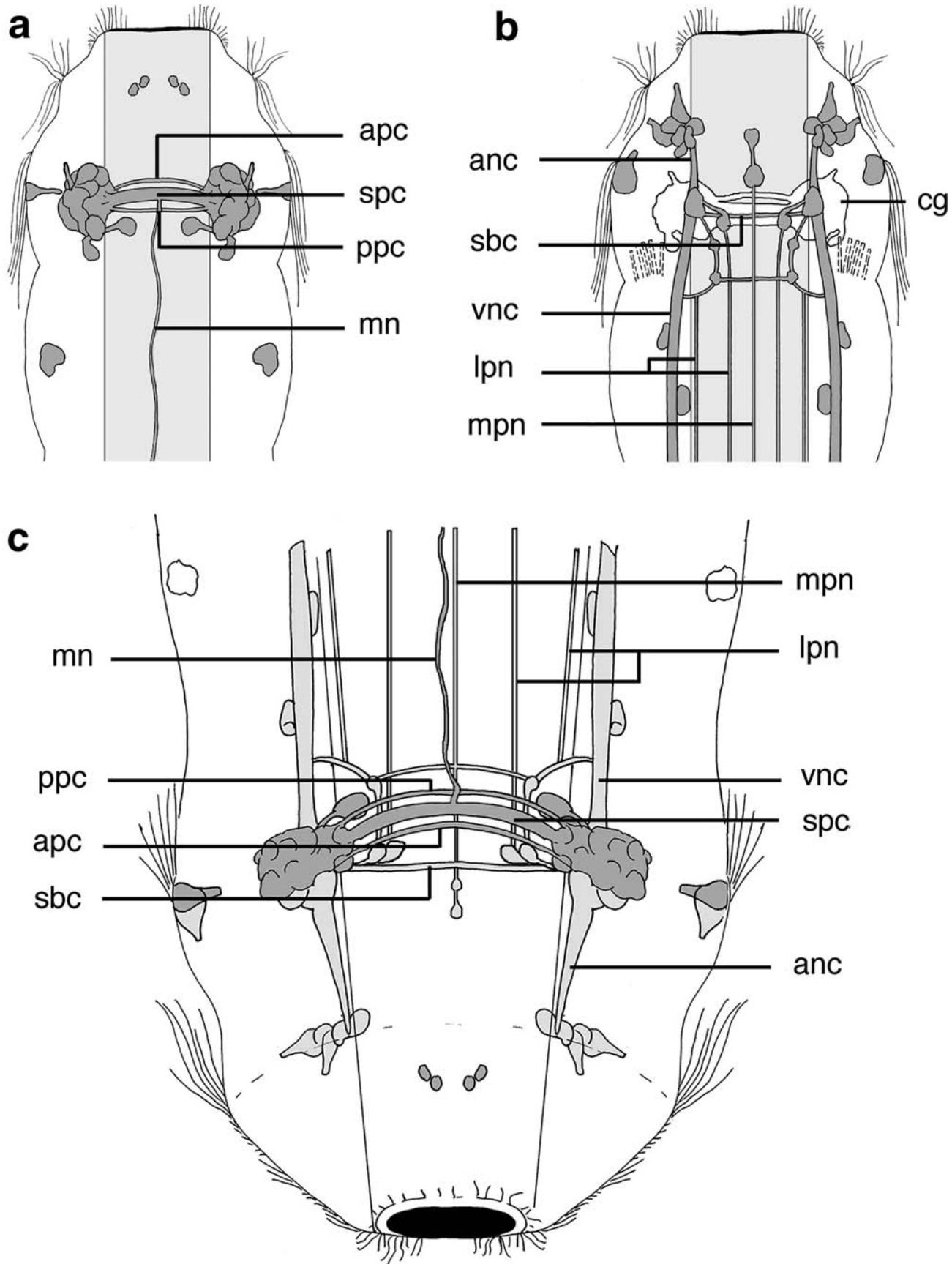
a
apc
spc
ppc
mn
b
anc
sbc
vnc
lpn
mpn
cg
c
mpn
mn
lpn
ppc
vnc
apc
spc
sbc
anc

◀ **Fig. 8** Diagrams of FMRFamide-like IR observed in *Turbanella* cf. *hyalina*. **a** Dorsal view of the anterior end. **b** Ventral view of the anterior end. The dorsal aspect of the cerebral ganglion is outlined (*cg*). **c** 3D en face view of the anterior end. Dorsal cells and neurites are *shaded darker* than ventral cells and neurites in this illustration. *anc* anterior nerve cord of the CNS, *apc* anterior pharyngeal commissure of the cerebral ganglion, *lpn* lateral pharyngeal neuron of the SNS, *mn* medial neuron of the PNS, *mpn* medial pharyngeal neuron of the SNS, *ppc* posterior pharyngeal commissure of the cerebral ganglion, *sbc* subpharyngeal commissure of the cerebral ganglion, *spc* suprapharyngeal commissure of the cerebral ganglion, *vnc* ventral nerve cord of the CNS

Two pairs of neurites (lpn) are present on either side of the pharynx and originate close to the base of the cerebral ganglion (Figs. 6d, 8b). Of each pair of neurites, the medial pair originates from a perikaryon close to the subpharyngeal commissure. These neurites terminate at the base of the pharynx. The lateral pair of neurites is more difficult to trace, but appear to originate from an interconnected series of shorter neurites that extend from the base of the cerebral ganglion posteriorly to the ventral nerve cords (Figs. 6d, 8). These neurites extend to the posterior end of the body (as lateral intestinal neurites, lin) and coalesce (Fig. 7b). Medially, a single neurite (mpn) originates from each bilateral perikaryon at the pharynx midline; this neurite extends past the pharyngeointestinal junction (as a medial intestinal neurite, min) and terminates in the posterior body region.

Neodasys cirritus (Chaetonotida: Multitubulatina)

The CNS shows strong IR within both the cerebral ganglion and nerve cords (Figs. 9, 10, 11). Measurements are taken from a single adult specimen approximately 310 µm long. The cerebral ganglion is located approximately 65 µm from the tip of the head and consists of a bilateral cluster of perikarya positioned around a central commissure (Figs. 9 b, 10, 11a). The cerebral ganglion measures approximately 39 µm wide and 30 µm long. Dorsally, there are three closely spaced commissures: a thin anterior pharyngeal commissure (1–2 µm diameter; apc, Figs. 10a, 11a, 12), a thick suprapharyngeal commissure (5–6 µm diameter; spc, Fig. 10a, b), and a thin posterior pharyngeal commissure (1–2 µm diameter; ppc, Figs. 10a, 12). The anterior commissure is lined with a few small perikarya (ca. 2–3 µm). The suprapharyngeal commissure is moderately convex (Fig. 10c, d). Approximately 25 bilateral perikarya are present on either side of the commissure. Most of these perikarya are located lateral and posterolateral to the suprapharyngeal and posterior pharyngeal commissures (Figs. 9b, 10, 11a). Individual perikarya are teardrop or oval in shape and approximately 3 µm wide by 5–6 µm long. There are no ventral perikarya and there is no subpharyngeal commissure.

Three pairs of nerve cords project off the cerebral ganglion. A single pair of dorsal nerve cords lined with perikarya project anteriorly along the pharynx for approximately 30 µm (anc, Figs. 10a, b, 11a). Posteriorly, two pairs of nerve cords project into the trunk region (Figs. 9, 10, 11). The nerve cords are ventrolateral (vlnc) and ventral (vnc) in position and appear to coalesce at the base of the trunk in a short commissure (not shown). Several IR cells are present in the pharyngeal and trunk regions (Figs. 9b, c, 10d, 11). All cells are teardrop shaped and approximately 3–4 µm wide by 5–6 µm long. It is undetermined if these perikarya are associated with the ventral or ventrolateral nerve cords (see Fig. 11a, b). There is no IR associated with perikarya or neurites outside of the CNS aside from those cells already described.

Discussion

General account

This study provides the first account of FMRFamide-like IR in the cerebral ganglion of gastrotrichs, and reveals the utility of immunoreagents for visualizing the general organization of the CNS, PNS and SNS. More specifically, results show that FMRFamide-like IR is present throughout the cerebral ganglion, in both cerebral perikarya and the neuropil (commissures), and that there are significant qualitative similarities among species from both major clades, Chaetonotida and Macrodasyida. Moreover, the distribution of FMRFamide-like IR differs substantially from the distribution of other neurotransmitters such as the biogenic amines, which are known in some detail for *Turbanella cornuta* (Joffe and Kotikova 1987; Joffe and Wikgren 1995), but only in a piecemeal fashion for other macrodasyidans (Hochberg and Litvaitis 2003). In general, FMRFamide-like IR is much more prevalent throughout the gastrotrich nervous system than is 5-HT, which is restricted to the CNS and found in a limited number of cerebral cells. In contrast, catecholamine histofluorescence is prevalent throughout the CNS, PNS and parts of the SNS, at least for *T. cornuta*, but is still comparatively more restricted than FMRFamide-like IR (see Joffe and Kotikova 1987).

Central nervous system

To date, knowledge of the gastrotrich cerebral ganglion is derived from a few studies, namely, ultrastructural investigations of *Turbanella cornuta* (Teuchert 1977) and *Cephalodasys maximus* (Wiedermann 1995), histochemical investigations of *Turbanella* sp. (Joffe and Kotikova 1987), and immunohistochemical investigations of *Turbanella cornuta* (Joffe and Wikgren 1995), *Dactylopodola baltica*

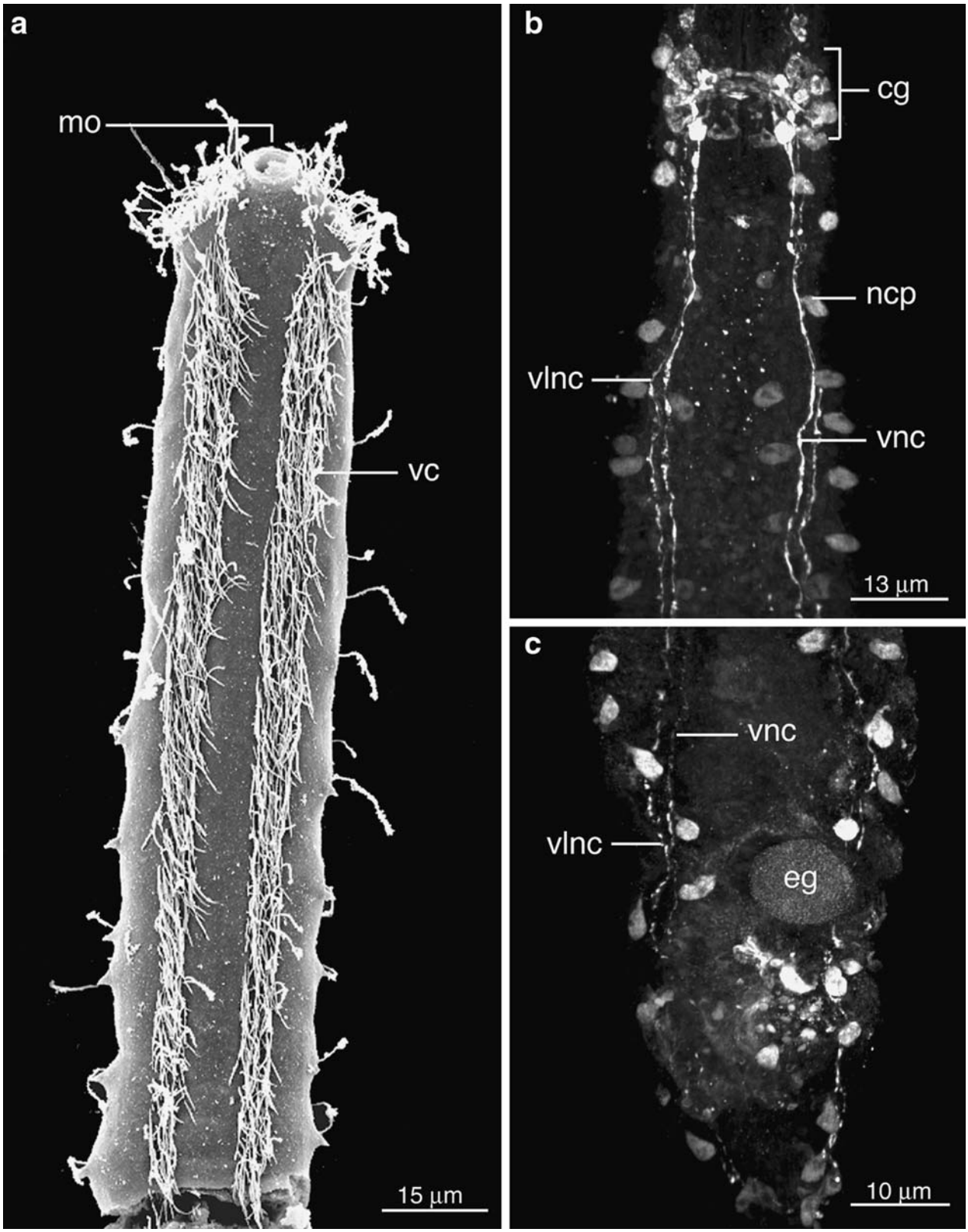

Fig. 9 SEM and confocal views of *Neodasys cirritus*. **a** anterior end in ventral view. **b** *Z*-projection of FMRFamide-like IR in the anterior end showing elements of the CNS (150 × 0.1 µm optical slices). **c** *Z*-projection of FMRFamide-like IR in the posterior end (162 × 0.1 µm optical slices). *cg* cerebral ganglion, *eg* ovum, *mo* mouth, *ncp* IR perikarya of the posterior nerve cords, *vc* ventral locomotory cilia, *vnc* ventral nerve cord of the CNS, *vlnc* ventrolateral nerve cord of the CNS

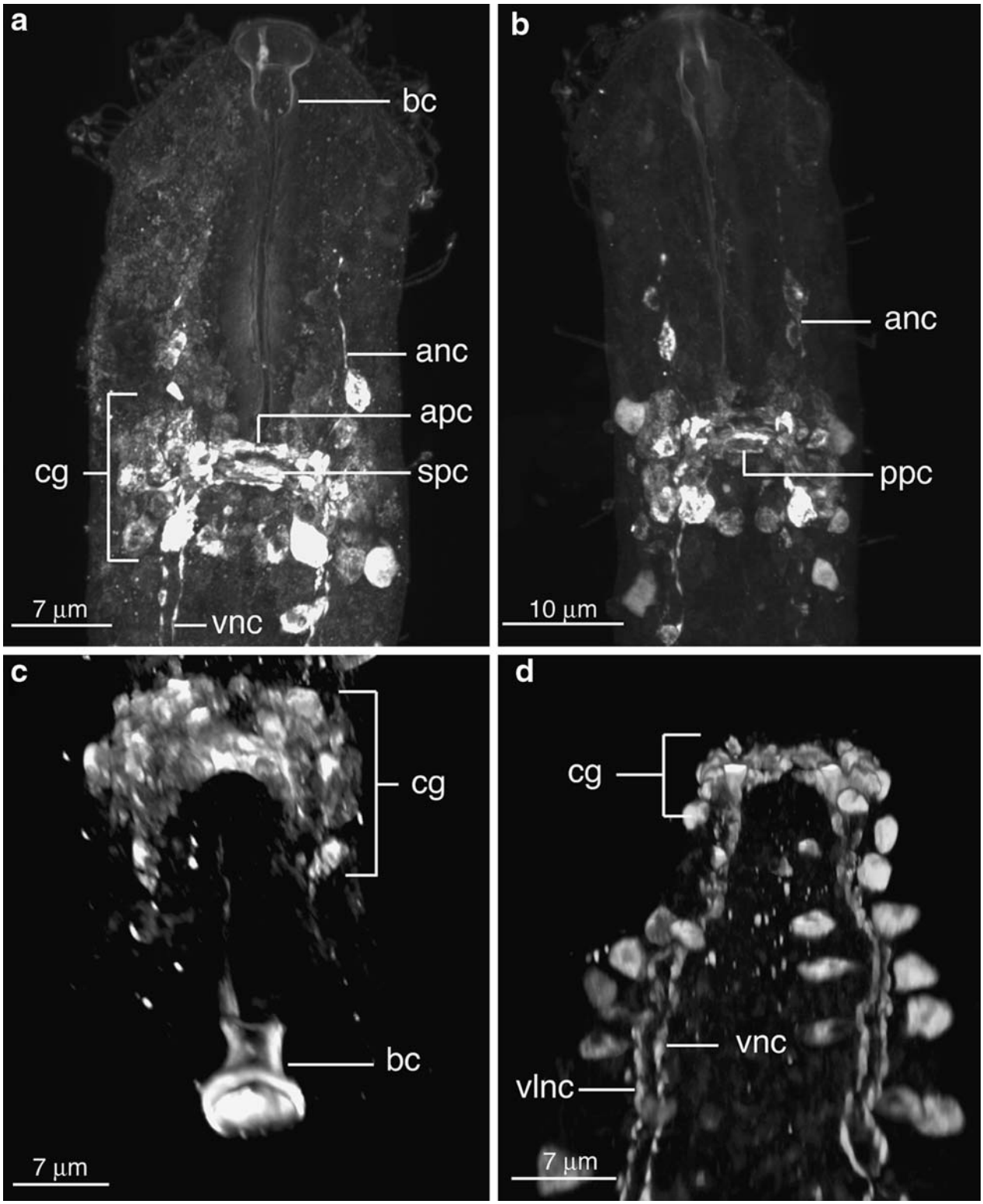

Fig. 10 Confocal and 3D images of FMRFamide-like IR in the anterior end of *Neodasys cirritus*. **a** *Z*-projection of the anterior end showing the anterior (*apc*) and suprapharyngeal commissures (*spc*) and perikarya of the cerebral ganglion (*cg*) 156 × 0.1 µm optical slices. **b** *Z*-projection of the anterior end (different specimen) showing the posterior pharyngeal commissure (*ppc*) of the cerebral ganglion and the anterior nerve cords (*anc*) 345 × 0.05 µm optical slices. **c** 3D en face view of the anterior end. The cuticular buccal capsule (*bc*) is autofluorescent. **d** View of the anterior region of the CNS from a dorsal position along the posterior trunk. *vlnc* ventrolateral nerve cord of the CNS, *vnc* ventral nerve cord of the CNS

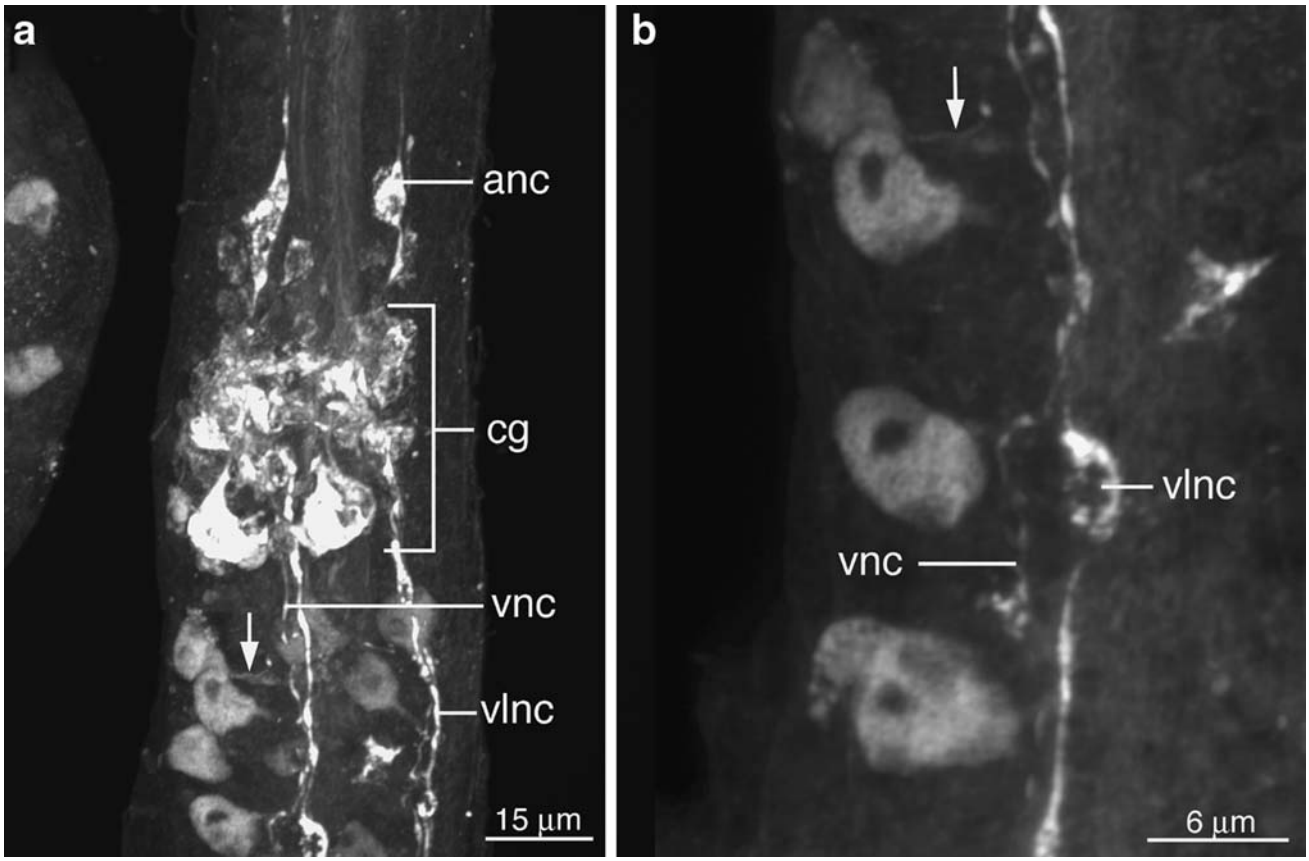

Fig. 11 *Z*-projections of FMRFamide-like IR in the perikarya associated with the cerebral ganglion (*cg*) and posterior nerve cords of *Neodasys cirritus*. **a** Mid-pharyngeal region showing the close association of perikarya with anterior nerve cords (*anc*) and the ventrolateral (*vlnc*) and ventral nerve cords (*vnc*) of the CNS. *Arrow* points to neural process that extends towards the nerve cords (239 × 0.1 µm) optical slices. **b** Closeup of perikarya in the trunk region. It is undetermined which nerve cord receives innervation from the perikarya (66 × 0.05 µm) optical slices

(Hochberg and Litvaitis 2003; Liesenjohann et al. 2006), and *Dolichodasys elongatus* and *Macrodasys caudatus* (Hochberg and Litvaitis 2003). Based on the ultrastructural investigations of *T. cornuta* and *C. maximus*, the cerebral ganglion is circumpharyngeal in construction, with a central neuropil constructed of a thick suprapharyngeal commissure and thin subpharyngeal commissure. Perikarya are distributed equally around the dorsal, lateral, and ventrolateral borders, and cover a series of anterior and posterior nerves that project from the neuropil. According to Teuchert (1977), cerebral perikarya are more-or-less regionally specialized along the anterior–posterior axis of the cerebral ganglion. For example, cells of different construction (e.g., volume, shape, amount of ER, size of nucleus, etc.) are hypothesized to have different functions, and are so named differently, beginning with d-cells at the anterior end and proceeding through k-cells in the posterior region. If indeed such regionalization is characteristic of the gastrotrich cerebral ganglion in general, then immunostaining may reflect this regionalization by revealing functionally different perikarya along the anterior-posterior axis. This may in fact be the case for the species examined in the current study: *X. riedli*, *T.* cf. *hyalina*, and *N. cirritus*. All three species show characteristic FMRFamide-like IR in small bilateral clusters of perikarya on either side of the neuropil—giving the cerebral ganglion a dumbbell shape—and corresponding to the region in *T. cornuta* that specifically contains c-cells, h-cells and i-cells (see Teuchert 1977). The fact that few IR perikarya are present outside of this dumbbell-shaped cluster, where cerebral perikarya should be prevalent (according to studies on other species), suggests that regional specialization of neurotransmitters is indeed present. Moreover, the neuropil also reflects this regional specialization by containing IR fibers in apparently separate (albeit very close) anterior and posterior pharyngeal commissures in some species. Future ultrastructural studies that utilize immunogold reagents should help clarify this apparent regionalization.

While the current study confirms many aspects of cerebral architecture in gastrotrichs, including its circumpharyngeal construction, convex shape, and the development of the commissures, the results are equivocal regarding the

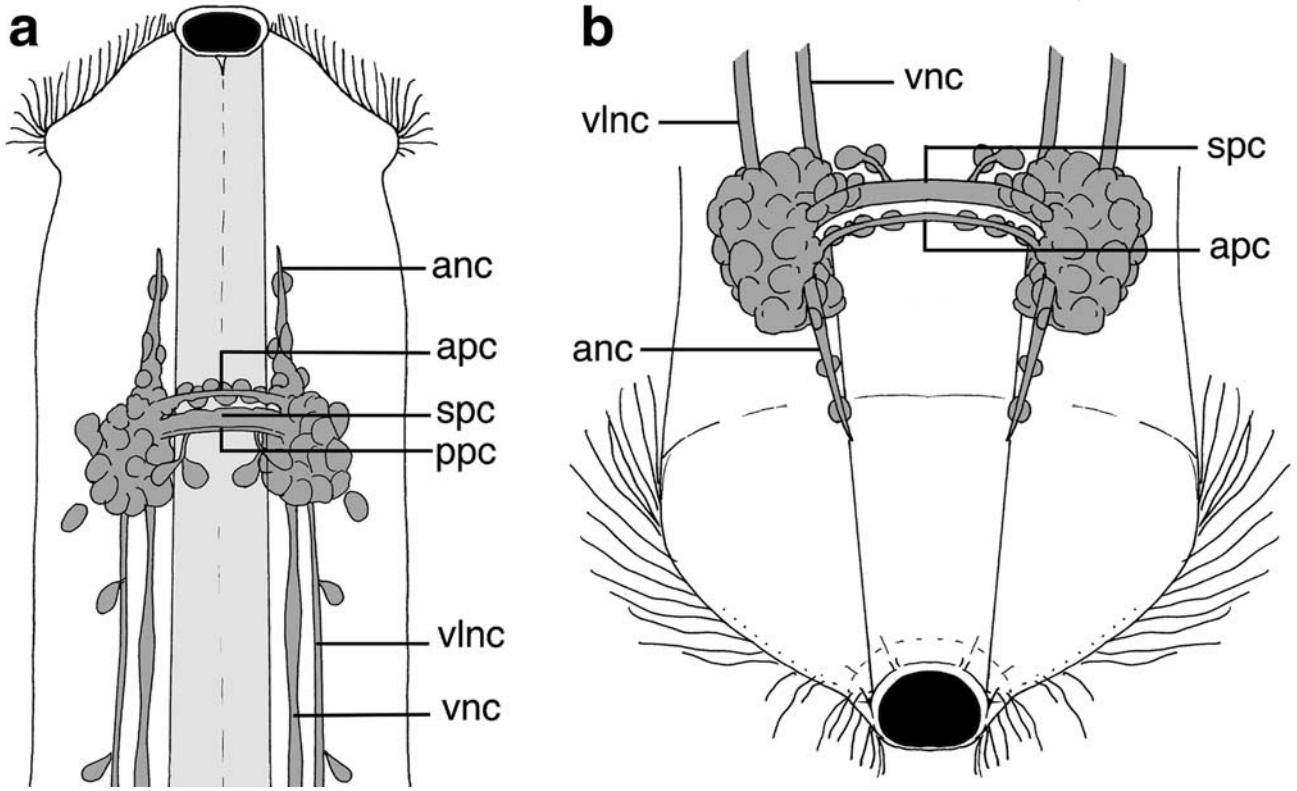

Fig. 12 Diagrams of FMRFamide-like IR observed in *Neodasys cirritus*. **a** Dorsal view of the anterior end. There is no IR in the PNS or SNS. **b** 3D en-face view of the anterior end. *anc* anterior nerve cord, *apc* anterior pharyngeal commissure, *ppc* posterior pharyngeal commissure, *spc* suprapharyngeal commissure, *vnc* ventral nerve cord, *vlnc* ventrolateral nerve cord

use of FMRFamide-like IR in understanding broad phylogenetic hypotheses. For example, Gastrotricha is hypothesized to be closely related to the Cycloneuralia, i.e., as a basal taxon within Cycloneuralia (Nielsen 1995) or as the sister taxon to Cycloneuralia (Schmidt-Rhaesa 1996). Both hypotheses employ the structure of the cerebral ganglion as a phylogenetic character to argue for the placement of the Gastrotricha. Nielsen (1995) hypothesizes that gastrotrichs, like all cycloneuralians, possess a tripartite cerebral ganglion (perikarya-neuropil-perikarya); Schmidt-Rhaesa (1996) argues that the distribution of cerebral perikarya in gastrotrichs is more diffuse and therefore different from species of Cycloneuralia *sensu strictu*. While the current results show that IR perikarya are clustered into distinct dumbbell-shaped zones around the neuropil, their position neither supports nor contradicts either hypothesis, especially in light of ultrastructural studies which show a more diffuse distribution of perikarya across the cerebral ganglion (Teuchert 1977; Wiedermann 1995). Unfortunately, the distribution of equivalent FMRFamidergic perikarya in most other cycloneuralians, with the exception of *Caenorhabditis elegans* (Nematoda), is unknown. Immunolocalization of FaRPs in *C. elegans* reveals IR in the neuropil and associated cells (Schinkmann and Li 1992), but no dumbbell shape is evident, and so the results are difficult to compare with those observed in gastrotrichs. Additional data on other nematodes, and other cyloneuralians, will help clarify whether patterns of FMRFamide-like IR in the cerebral ganglion can be used as a phylogenetic character in support of these hypotheses.

While the structure of the cerebral ganglion was the focus of the current study, immunohistochemical analysis also revealed several details about the major nerve cords, elements of the PNS, and innervation of the myoepithelial pharynx. Regarding the major nerve cords, this study confirms earlier hypotheses that suggest that species in potentially basal clades, e.g., *N. cirritus* of Multitubulatina (Chaetonotida) and *X. riedli* of Xenodasyidae (Macrodasyida), possess multiple nerve cords. For example, Travis (1983) hypothesized that multiple nerve cords (>2) are the plesiomorphic condition in Gastrotricha (based on their presence in *D. baltica* and a species of *Neodasys*), as it is for other bilaterians (see Bullock and Horridge 1965; Orrhage and Müller 2005). The current analysis therefore confirms the basal position of species of *Neodasys* within the Chaetonotida. Likewise, the results also attest to the basal position of *Xenodasys*, a group of gastrotrichs that once shared taxonomic propinquity to other basal macrodasyidans based on the retention of plesiomorphic characteristics (as members of the Dactylopodolidae, see

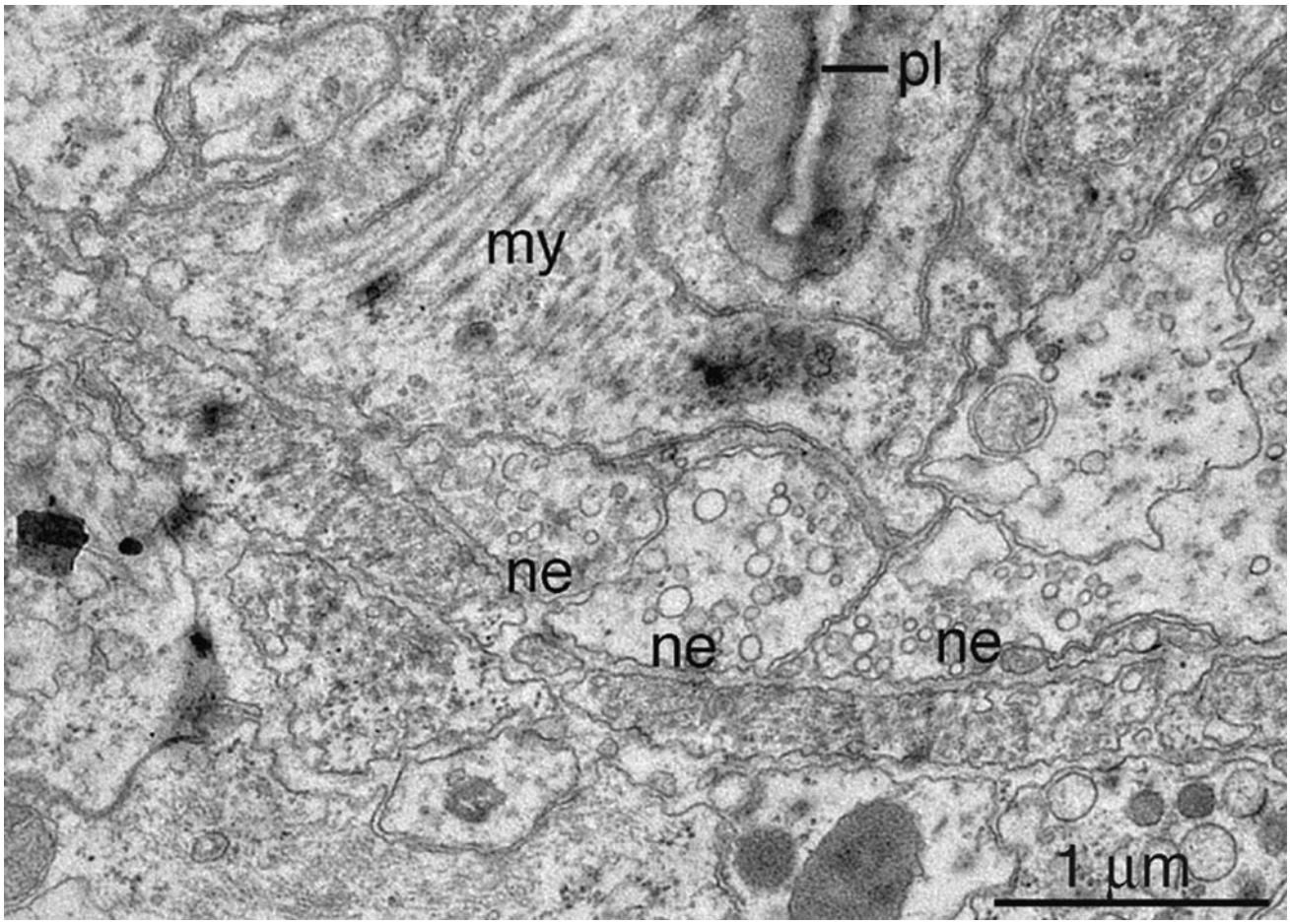

Fig. 13 **a** TEM micrograph of the ventral pharyngeal region of *Dactylopodola baltica* showing a bundle of neurites (*ne*) with numerous vesicles. *my* mypepithelial cell, *pl* pharyngeal lumen surrounded by cuticle

Hochberg and Litvaitis 2001), but are now recognized as members of a separate taxon (Xenodasyidae, Todaro et al. 2006). Furthermore, these results place species of *Xenodasys* in a basal position relative to other members of Xenodasyidae, e.g., species of *Chordodasiopsis* (the senior synonym of *Chordodasys*), which are known to possess only a single pair of major nerve cords (see Rieger et al. 1974).

Peripheral and stomatogastric nervous system

The PNS and SNS of gastrotrichs are known mostly from ultrastructural investigations, with perhaps the most detailed information coming from a study of *C. maximus* (Wiedermann 1995). In her study, Wiedermann revealed that *C. maximus* has a much more complicated SNS than previously revealed in other species (see Ruppert 1982). In particular, *C. maximus* possesses a pharyngeal nerve ring that gives rise to several anterior and posterior nerves, some of which innervate various sensory receptors in the pharynx, and others that connect to the rest of the nervous system. The difference in the number of pharyngeal nerves in *C. maximus* and that observed in other species by Ruppert (1982) may be an artifact, since the latter investigation did not employ serial sections that may otherwise have detected additional neurons. Likewise, immunohistochemistry is also artifactual in the sense that only a few of the pharyngeal neurons are revealed based on their IR, and therefore difficult to homologize with nerves visualized with TEM. Moreover, pharyngeal nerves often represent bundles of individual neurons (see Fig. 13; also Ruppert 1991); if each neuron possesses a different IR, then immunostaining will only reveal a piecemeal picture. Yet, neuronal homology may still be possible based on positional correspondence of similar IR cells among species. For example, both macrodasyidans in the current study possess one median (mpn) and two lateral pharyngeal neurites (lpn), with *T.* cf. *hyalina* possessing an additional pair of mediolateral pharyngeal neurites. Whether these additional neurons contribute to differences in pharyngeal function, or have systematic implications, remains to be determined. Perhaps even more curious is the total absence of IR in the

pharynx of *N. cirritus*. FMRFamide and FARPS are well known to have myotropic effects on nematode muscles, most notably, the pharyngeal myoepithelium, where they inhibit pharyngeal contractions (Rogers et al. 2001). Assuming a similar inhibitory function of FMRFamide-like peptides for gastrotrich pharynges—Ruppert (1982) notes that the chaetonotidan pharynx is more similar to that of nematodes than to macrodasyidans—it would be interesting to know how *N. cirritus* inhibits pharyngeal contraction, or if other chaetonotidans show a similar lack of IR in their pharynges.

Conclusions

The gastrotrich nervous system has been the subject of relatively few investigations, but results revealed in earlier ultrastructural analyses, combined with the current immunohistochemical insights, provides a growing picture of some of the neuronal complexity in these microscopic worm-like invertebrates. Additional species, representing a much wider taxonomic range, would greatly increase our knowledge of nervous system structure and function, and provide us a better idea of the utility of the nervous system for understanding gastrotrich phylogeny. The realization that neural architecture is much more conserved than other organ systems has been known for some time (e.g., Bullock and Horridge 1965) and has provided the basis for using neural characters in phylogenetic analysis, i.e., neurophylogeny (Harszch 2002). This concept has received significant attention within Arthropoda (see Harzsch and Waloszek 2000; Harszch 2002, 2006; Paul 2003) and Annelida to a lesser degree (references in Orrhage and Müller 2005), but has been largely ignored in many other metazoans including gastrotrichs. The structure of the gastrotrich cerebral ganglion, despite its miniscule size, has the potential to provide keen insights into relationships with other taxa such as the lophotrochozoans. For example, immunohistochemistry reveals an intriguing bilobed distribution of FMRFamide-like IR in the gastrotrich cerebral ganglion—a condition very similar to that observed in other presumably unrelated animals, e.g., the chordoid larva of cycliophorans (Wanninger 2005) and species of Entoprocta (Fuchs et al. 2006). Is this distribution of IR cells evidence of an ancestral, bilobed condition for the protostome cerebral ganglion? Moreover, is the gastrotrich condition, characterized by additional non-IR perikarya (based on EM studies) superimposed upon this dumbbell-shaped cerebral ganglion, evidence of a more derived condition? Further research is clearly necessary to answer such questions and provide a better understanding of cerebral architecture in species of Gastrotricha.

Acknowledgments The author is grateful for the comments by two anonymous reviewers that improved this manuscript. The author is also grateful to the staff at the Smithsonian Marine Station in Fort Pierce, Florida for their assistance in collection and the use of their facilities. This research received financial support from the University of Massachusetts Lowell and from the Sumner Gerard Foundation at the Smithsonian Marine Station at Fort Pierce, Florida. This is Smithsonian Marine Station at Fort Pierce contribution 706.

References

Bullock TH, Horridge GA (1965) Structure and function in the nervous system of invertebrates, vols I, II. WH Freeman, San Francisco

Burry RW (2000) Specificity controls for immunocytochemical methods. J Histochem Cytochem 48:163–165

Fuchs J, Bright M, Funch P, Wanninger A (2006) Immunocytochemistry of the neuromuscular systems of *Loxosomella vivipara* and *L.* parguerensis (Entoprocta: Loxosomatidae). J Morphol 267:866–883

Gagné GD (1980) Ultrastructure of the sensory palps of *Tetranchyroderma papii* (Gastrotricha, Macrodasyida). Zoomorphologie 95:115–125

Garey J (2001) Ecdysozoa: the relationship between Cycloneuralia and Panarthropoda. Zool Anz 240:321–330

Grimmelikhuijzen CJP (1983) FMRFamide immunoreactivity is generally occurring in the nervous systems of coelenterates. Histochem Cell Biol 78:361–381

Harszch S (2002) Neurobiologie und Evolutionsforschung: 'Neurophylogenie" und die Stammesgeschichte der Euarthropoda. Neuroforum 4:267–273

Harszch S (2006) Neurophylogeny: architecture of the nervous system and a fresh view on arthropod phylogeny. Integr Comp Biol 46:162–194

Harzsch S, Waloszek D (2000) Serotonin-immunoreactive neurons in the ventral nerve cord of Crustacea: a character to study aspects of arthropod phylogeny. Arthropod Struct Dev 29:307–322

Hochberg R, Litvaitis MK (2001) The musculature of *Dactylopodola baltica* and other macrodasyidan gastrotrichs in a functional and phylogenetic perspective. Zool Scr 30:325–336

Hochberg R, Litvaitis MK (2003) Ultrastructural and immunocytochemical observations of the nervous systems of three macrodasyidan gastrotrichs. Acta Zool 84:171–178

Joffe BI, Kotikova EA (1987) Catecholamines in the nervous system of the gastrotrich *Turbanella* sp. Dokl Akad Nauk SSSR 296:1509–1511

Joffe BI, Wikgren M (1995) Immunocytochemical distribution of 5-HT (serotonin) in the nervous system of the gastrotrich *Turbanella cornuta*. Acta Zool 76:7–9

Krajniak KG (2005) Annelid endocrine disruptors and a survey of invertebrate FMRFamide-related peptides. Integr Comp Biol 45:88–96

Lehman HK, Price DA (1987) Localization of FMRFamide-like peptides in the snail *Helix aspersa*. J Exp Biol 131:37–53

Liesenjohann T, Neuhaus B, Schmidt-Rhaesa A (2006) Head sensory organs of *Dactylopodola baltica* (Macrodasyida, Gastrotricha): a combination of transmission electron microscopical and immuncytochemical techniques. J Morphol 267:897–908

Müller MCM, Sterrer W (2004) Musculature and nervous system of *Gnathostomula peregrina* (Gnathostomulida) shown by phalloidin labeling, immunohistochemistry, and CLSM, and their phylogenetic significance. Zoomorphology 123:169–177

Nichols R, McCormick JB, Lim IA (1999) Structure, function, and expression of *Drosophila melanogaster* FMRFamide-related peptides. Ann NY Acad Sci 897:264–72

Nielsen C (1995) Animal evolution. Oxford University Press, Oxford
Orrhage L, Müller MCM (2005) Morphology of the nervous system of Polychaeta (Annelida). Hydrobiologia 535/536:79–111
Price DA, Greenberg MJ (1977) Structure of a molluscan cardioexcitatory neuropeptide. Science 197:670–671
Paul DH (2003) Neurobiology of the Anomura: Paguroidea, Galtheiodea and Hippoidea. Mem Mus Vic 60:3–11
Rieger RM, Ruppert EE, Rieger GE, Schoepfer-Sterrer C (1974) On the fine structure of gastrotrichs, with a description of *Chordodasys antennatus* sp. n. Zool Scr 3:219–237
Rogers CM, Franks CJ, Walker RJ, Burke JF, Holden-Dye L (2001) Regulation of the pharynx of *Caenorhabditis elegans* by 5-HT, octopamine, and FMRFamide-like neuropeptides. J Neurobiol 49:235–244
Ruppert EE (1982) Comparative ultrastructure of the gastrotrich pharynx and the evolution of myopeithelial foreguts in Aschelminthes. Zoomorphology 99:181–220
Ruppert EE (1991) Gastrotricha. In: F Harrison, E.E. Ruppert (Eds) Microscopic anatomy of invertebrates, vol 4, Aschelminthes. Wiley, Washington, pp 41–109
Schinkmann K, Li C (1992) Localization of FMRFamide-like peptides in *Caenorhabditis elegans*. J Comp Neurol 316:251–260
Schmidt-Rhaesa A (1996) The nervous system of *Nectonema munidae* and *Gordius aquaticus*, with implications for the ground pattern of the Nematomorpha. Zoomorphology 116:133–142
Shaw C, Maule AG, Halton DW (1996) Platyhelminth FMRFamide-related peptides. Int J Parasitol 26:335–45
Teuchert G (1976) Sinneseinrichtigungen bei *Turbanella cornuta* Remane (Gastrotricha). Zoomorphologie 83:193–207
Teuchert G (1977) The ultrastructure of the marine gastrotrich *Turbanella cornuta* Remane (Macrodasyoidea) and its functional and phylogenetic importance. Zoomorphologie 88:189–246
Todaro MA, Guidi L, Leasi F, Tongiorgi P (2006) Morphology of *Xenodasys* (Gastrotricha): the first species from the Mediterranean Sea and the establishment of *Chordodasiopsis* gen. nov. and Xenodasyidae fam. nov. J Mar Biol Assoc UK 86:1005–1015
Travis PB (1983) Ultrastructural study of body wall organization and Y-cell composition in the Gastrotricha. Z Zool Syst Evol 21:52–68
Wanninger A (2005) Immunocytochemistry of the musculature and the nervous system of the chordoid larva of *Symbion pandora* (Cycliophora). J Morphol 255:237–243
Wiedermann A (1995) Zur Ultrastruktur des Nervensystems bei *Cephalodasys maximus* (Macrodasyida, Gastrotricha). Microfauna Mar 10:173–233